Development of Finite Element Model for Charring Rate for Solid Timber from Malaysian Tropical Hardwood Subjected to Standard Fire

Lannie Francis,[a,b] Ahmad Beng Hong Kueh,[c,d] Norshariza Mohamad Bhkari,[a,e] Hafizah Muhamad Azlan,[a] and Zakiah Ahmad,[a,*]

Timber has natural fire resistance because of its predictable charring behavior. When subjected to high temperatures, timber undergoes pyrolysis, forming an insulating char layer that protects the inner structural core. Eurocode EN 1995-1-2 (2004), commonly known as Eurocode 5 where EC5 specifies 0.5 mm/min charring rate for temperate hardwoods, pertains to timber with density exceeding 450 kg/m³. This paper presents the development of a finite element model (FEM) to predict the charring rate of timber exposed to fire through innovative experimental and numerical approaches. Timber samples were exposed to controlled heat fluxes for 60 min, simulating real-world fire scenarios. The resulting char layer thickness was measured over time. The Malaysian tropical hardwood timber used was Resak (*Cotylelobium* and *Vatica* spp.) with density range from 932 kg/m^3 to 1125 kg/m^3. The proposed FEM was developed using ABAQUS software, which included thermal conductivity and specific heat to simulate the transient heat transfer and degradation processes in timber. It was found that the charring rate of Resak was 0.47 mm/min lower than the rates established in EC5 (2004). The model is validated through experimental data, demonstrating its accuracy in predicting char depth and temperature profiles under standard fire condition. The data are useful when designing the fire safety of timber structures from the Malaysian tropical timber species.

DOI: 10.15376/biores.20.3.7695-7712

Keywords: Tropical hardwood timber; Charring rate; Numerical analysis; Finite element model; Pyrolysis; Fire resistance

*Contact information: a: Faculty of Civil Engineering, Universiti Teknologi MARA, 40450 Shah Alam, Selangor, Malaysia; b: Faculty of Civil Engineering, Universiti Teknologi MARA, Sarawak Branch, Kota Samarahan Campus, 94300 Kota Samarahan, Sarawak, Malaysia; c: Department of Civil Engineering, Faculty of Engineering, Universiti Malaysia Sarawak, 94300 Kota Samarahan, Sarawak; d: UNIMAS Water Centre (UWC), Faculty of Engineering, Universiti Malaysia Sarawak, 94300 Kota Samarahan, Sarawak, Malaysia; e: Institute for Infrastructure Engineering and Sustainable Management (IIESM), Universiti Teknologi MARA, 40450 Shah Alam, Selangor, Malaysia; *Corresponding author: zakiah@uitm.edu.my*

INTRODUCTION

The use of timber as a construction material has experienced a resurgence in recent years, driven by its sustainability, aesthetic appeal, and low carbon footprint. However, as timber is a combustible material, understanding its behavior under fire exposure is critical for ensuring the safety and structural integrity of timber buildings. A key characteristic that influences the fire performance of timber is its charring rate, which refers to the rate at which the material degrades when subjected to elevated temperature. Timber undergoes pyrolysis when exposed to high temperatures, a process that leads to the formation of a char layer on the surface of the material. This char layer plays a significant role in protecting the unburned timber beneath it by acting as an insulating barrier, reducing the rate of heat transfer to the core of the structural element and weight loss and cross-section (Li *et al.* 2015). It has been reported that the charring forms a layer of char on the timber element when the wood surface is exposed to fire temperatures as low as 260 °C, with 300 °C temperature being the specification of the European design code for timber building (EC5 2004; Suzuki *et al*. 2016). The temperature of 300 °C represented by the isotherm is generally a good indication of the location of charring depth and charring (White and Dietenberger 2001; Frangi *et al*. 2008). The charring rate of timber is typically calculated by measuring the char depth and dividing it by the time of fire exposure. This method is widely used in fire resistance assessments and research studies on timber charring behaviour (Liu *et al*. 2024). Research confirms that the rate of charring depends on various factors, including the type of timber, its moisture content, density, and the fire's intensity (Bartlett *et al.* 2019; Gan *et al*. 2019; Tanui *et al*. 2020; Albert and Liew 2023). Eurocode 5 (EC5), which deals with the fire design of timber structures, provides guidance on determining charring rates and the subsequent fire resistance of timber elements (EC5 2004).

Traditionally, the charring rate of timber has been studied through experimental fire tests, which, while providing valuable insights, are costly, time-consuming, and limited in the range of variables they can explore. To overcome these limitations, numerical methods and computational models have been developed to simulate the charring process and provide more versatile tools for fire safety engineers. Among these approaches, the Finite Element Method (FEM) has emerged as a powerful technique for modelling the complex heat transfer and degradation processes in timber exposed to fire. The investigation of charring rate of timber when exposed to fire have been experimentally and numerically carried out in different countries by many researchers in the past decades (Tran *et al*. 2020; Pecenko *et al.* 2023; Amin *et al*. 2024; Alanen *et al*. 2024; Li *et al.* 2024; Khelifa *et al.* 2024).

A key challenge in modeling the charring rate of timber lies in the accurate representation of material properties, which vary with temperature. As timber chars, its density, thermal conductivity, and specific heat capacity change. Early models often used constant thermal properties, leading to inaccuracies in predicting charring rates. Modern approaches incorporate temperature-dependent properties. The thermal conductivity's dependence on temperature is considered for the model development, which significantly improves prediction accuracy for timber char depth (Shi and Chew 2023). The boundary conditions, particularly the heat flux imposed on timber surfaces, also play a crucial role. The FEM allows for incorporation of complex boundary conditions, such as radiative and convective heat transfer, which are more challenging to implement in simpler numerical methods.

The charring rate is thus a critical factor in determining the fire resistance of timber structures. A precise understanding of this process allows for the accurate prediction of the load-bearing capacity and stability of timber elements during fire exposure, which is essential for performance-based fire design in modern construction.

There have been only few studies on experimental and numerical modelling of the charring rate of timber from Malaysian tropical hardwood. For example, Bakri (2023) described the new three predicted models, which were developed from statistical tools for laminated veneer lumber from different timber species and validated by the experimental results. Jabar (2023) conducted experimental investigation on charring rates of Malaysian Kelampayan timber and found that the charring rate is in the range of 0.77 mm/min to 0.84 mm/min. The study only focused on experimental works but was not validated with numerical analysis. There is a research gap observed from previous research on the use of timber materials especially from Malaysian timber for determining its thermal behaviour and charring rate. Determination of the thermal behaviour and charring rate of timber are mostly done by conducting experimental tests, and few studies have evaluated it numerically, especially with a numerical model developed using software.

Conducting individual species *via* experimental work is rather costly. Therefore, there is a need to develop model in predicting the charring rate of Malaysian tropical timber because Malaysia is blessed with more than 3000 timber species.

This study presents the development of a FEM approach for predicting the charring rate of tropical timber. Through developing an accurate and reliable tool for predicting timber behavior in fire, this research aims to contribute to the broader understanding of fire performance of timber and support the design of safer, more resilient timber structures.

EXPERIMENTAL

Preparation of Timber Materials

Resak (*Cotylelobium* spp. and *Vatica* spp.), which belongs to the *Dipterocarpaceae* family with density range of 932 kg/m^3 to 1125 kg/m^3, was selected for the study. The beams with dimensions of 100 mm (W) × 300 mm (H) × 1400 mm (L) were prepared. Timber specimen was supplied in a dry condition at less than 18% moisture content and visually graded based on standard grade in accordance with MS 1714 (2003). The grading is essential for ensuring that the timber specimens have a uniform grade to collect accurate data.

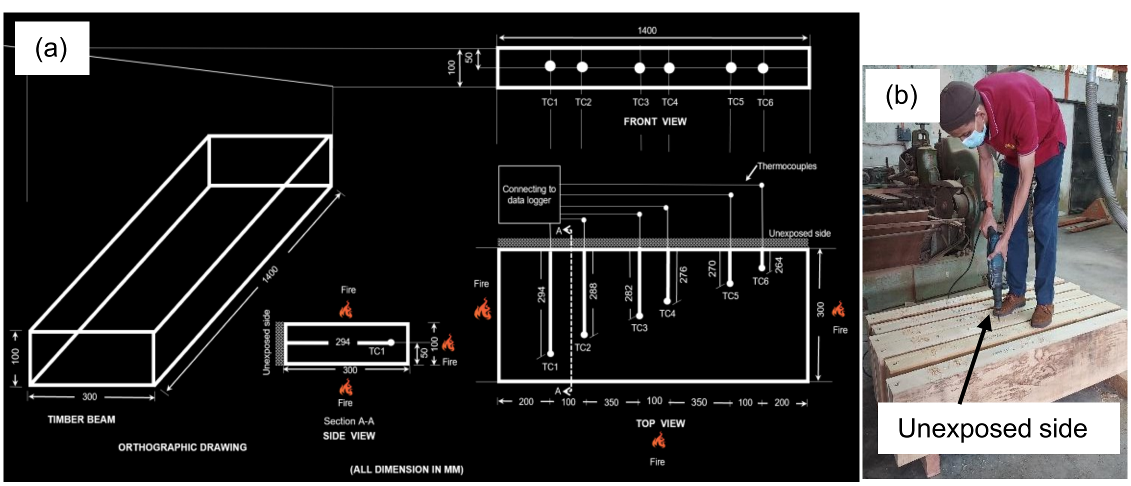

Fig. 1. Preparation of specimen: (a) Schematic diagram for thermocouple layout and (b) drilling holes on the marked positions of thermocouple at unexposed side

To mount the thermocouples into each beam, each specimen was marked for drilling process. The holes with diameter of 5 mm were drilled into the beam specimens at depths of 6, 12, 18, 24, 30, and 36 mm from the top edge surface not exposed to fire, and were designated as TC1, TC2, TC3, TC4, TC5, and TC6, respectively. This arrangement ensures comprehensive temperature readings, following the methodology outlined by König (2005). Figure 1(a) shows a schematic diagram of the thermocouple positions (TC1 to TC6) along the beam, while Fig. 1(b) illustrates the drilling process for inserting the thermocouples through the unexposed side. To prevent any slippage and movement of the thermocouples during the standard fire test, the thermocouples were securely installed inside the drilled hole of the timber. The holes were then sealed and surrounded by heat-resistance fire blanket. Type-K thermocouples of 4.8 mm diameter and with three different lengths; 100 mm, 200 mm, and 300 mm that can withstand up to 1200 ºC were used. The tip of the thermocouples was joined with a quick tip of diameter 2.5 mm. These thermocouples were connected to a data logger for temperature recording. Measurements were made from the thermocouples with a frequency of 0.2 Hz. These thermocouples were installed to verify it follows the necessary time-temperature curve, which is based on BS476: Part 20 (1987), comparable to EN 1363-1 (2012) and ISO 834 (2014).

Fire Test Set Up

The fire test was conducted at the Fire Laboratory at Forest Research Institute Malaysia (FRIM) using a gas-fired furnace that has dimensions of about 1500 mm × 1500 mm × 1500 mm. A special castable refractory cement-steel frame was fabricated to hold three specimens, as shown in Fig. 2(a). Rockwool was used to fill any gaps in the slots after placing the timber specimens. Figure 2(b) illustrates the parts of the specimens exposed to fire inside the furnace. Three beams were used for this fire test. The fire test was conducted following standard fire test procedures and specifications in accordance with BS476: Part 20 (1987).

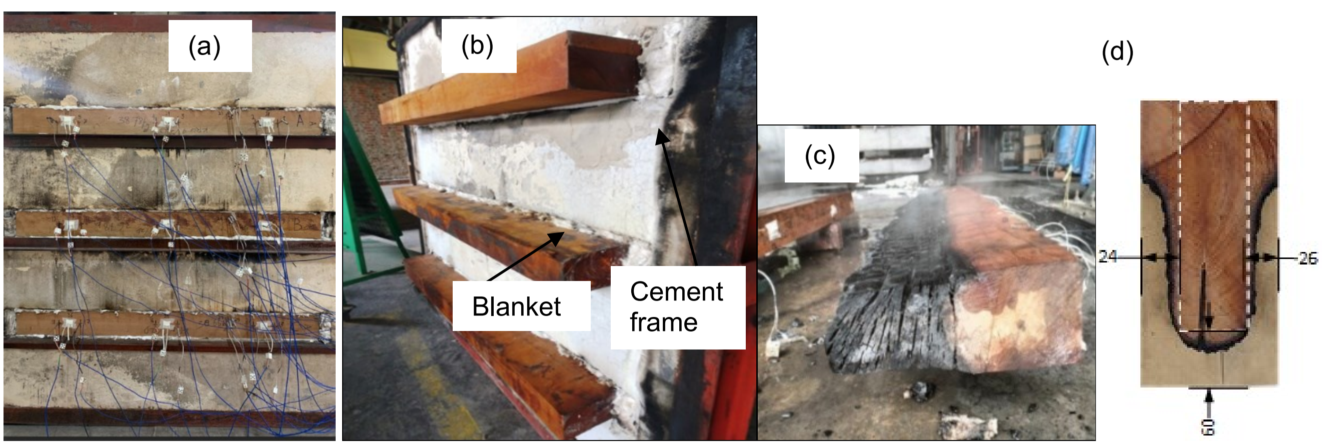

Fig. 2. Experimental specimen preparation: (a) specimens with attached thermocouples, b) specimen side exposed to fire, (c) Edge view after test, and (d) Comparison after removing the char

As required by Clause 213 of the Malaysian Uniform Building By-Laws 1984, structural elements must exhibit a fire resistance of more than 30 min (UBBL 1984). For this study, the specimens were exposed to fire for a duration of 60 min. At the end of fire test, all specimens were removed from furnace and extinguished with a dry powder fire extinguisher to stop the fire and then with water to stop the charring process. Figure 2 (c) and 2(d) show the specimen before and after fire test. In this study, the charring rate was determined using an indirect measuring approach in accordance with EN13381-7 (2019), which involved the temperature obtained from thermocouples (TC) at various depths (TC1 = 6 mm, TC2 = 12 mm, TC3 = 18 mm, TC4 = 24 mm, TC5 = 30 mm, TC6 = 36 mm) during the 60-min fire duration. This method provides exact information on the progression of charring throughout the fire test. The charring rate of timber, as accepted by the standard, begins at the 300 ºC isotherm. However, direct readings of the 300 ºC isotherm cannot be obtained from thermocouples. Therefore, it was determined by interpolation. The charring rate was calculated using Eq. 1. In this equation, d represents the char depth (mm), and t denotes the duration of exposure (minute).

$$\beta_n = \frac{d}{t} \tag{1}$$

Model Simulation

The ABAQUS finite element software program (Dassault Systèmes Simulia Corp., v.6.14, Providence, RI, USA) was used to analyse the thermal behaviour and charring of the timber element under fire condition. The ABAQUS is a computer-based program designed to simulate a wide range of engineering problems. For the numerical simulations, thermal analysis was adopted by incorporating the nonlinear behaviour of the materials coupled with the transient heat transfer. The following assumptions were considered in the numerical simulations, namely:

a) The samples are regarded as homogeneous.
b) The thermal behavior is considered isotropic, as there is no noticeable difference in thermal conductivity between the tangential and radial directions of the timber.

For an isotropic thermal and temperature dependent characteristic of timber, it is necessary to understand the heat transfer processes. The heat transfer development is based on the energy conservation equation as in Eq. 2,

$$\rho C\frac{\partial T}{\partial t} = \frac{\partial}{\partial x}\left[\lambda_x\frac{\partial T}{\partial x}\right] + \frac{\partial}{\partial y}\left[\lambda_y\frac{\partial T}{\partial y}\right] + \frac{\partial}{\partial z}\left[\lambda_z\frac{\partial T}{\partial z}\right] + Q_r'' \tag{2}$$

where T is the temperature (°C); λ_x, λ_y, and λ_z are the temperature-dependent thermal conductivities in the three directions, x, y, and z; ρ is the density (kg/m^3); C is the specific heat capacities (J·kg^{-1}·K^{-1}); and Q_r'' is the sum of reaction heat of the different pyrolysis reactions at the temperature field T, depending on the reaction rate, activation energy, and heat reaction of every pyrolysis reaction. This expression shows that the net amount of energy, transferred by conduction inside of the unit volume, for any point of the volumetric flow rate, is equal to the rate of change thermal energy stored within this volume.

The solid timber member cross-section models were developed using a heat transfer model in ABAQUS to simulate the fire test of timber members exposed to fire on three sides for 60 min, as shown in Fig. 2. The temperature-dependent thermal properties of the timber cross-sections used in numerical modeling followed EC5 (2004). After completing the input data for the material properties, including the heat conductivity, thermal capacity, and the density, a 3D thermal model was created in

ABAQUS using DC3D8 element (Abaqus 2014). A nonlinear transient analysis was employed as the primary step for heat transfer, as the temperature increased from room temperature to 300 °C for 3600 s, simulating the 60 min experimental fire exposure. The model used the furnace temperature taken from experimental work, with a minimum time interval of 0.1 s for each step. The thermal FEM for the three-sided fire exposure was developed by considering the three heat transfer mechanisms: radiation, conduction, and convection. In the first step of the analysis, a predefined field was established for the initial ambient temperature of 25 °C. The heat step was then applied to the model assembly using temperature data from the fire test thermocouples. The emissivity of the exposed surface of the timber model and the convection factor were assumed to be 0.8 and 25 W/m²K, as suggested by EC5 (2004). According to Trans *et al.* (2022), a convection coefficient of 25 W/m²K represents the heat transfer between the timber surface and the air in contact. A convection coefficient of 9 W/m²K was applied to the unheated side of the timber cross-section, assuming it was adiabatic. For this investigation, standard and linear geometric orders were selected for the element type. The 3D models were meshed with 42,000 elements and 48,081 nodes, using a global seed size of 0.01 mm. When using the finite element approach, a mesh convergence study was performed to see whether the analysis was correct and reliable. Figure 3 indicates that the temperature converged with a decreasing percentage difference of less than 1%, indicating that the model has achieved mesh convergence and is unaffected by mesh size changes. Once all models were properly designed and meshed, they were submitted for simulation analysis.

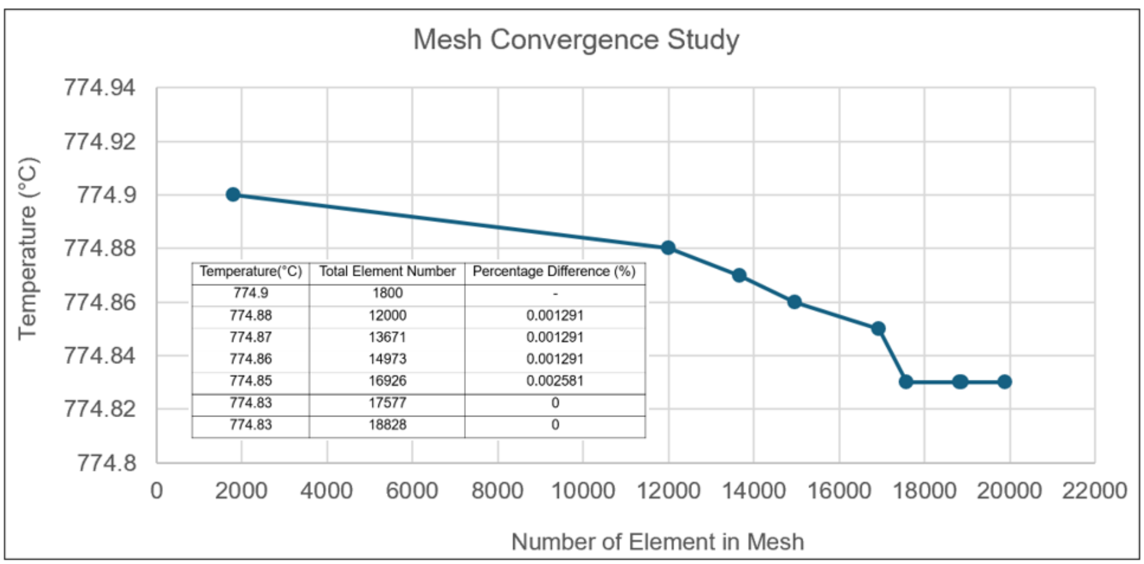

Fig. 3. Convergency study

Visualization of Temperature Distribution and Charring Rate

To identify the position of the 300 °C isotherm on the temperature contours and locate the formation of timber char, the contour value was set to a maximum of 300 °C, with the charred layer represented in grey after the analysis was successfully completed (Fig. 4).

Using nodal temperature (NT11) data from the temperature contour, a temperature-time curve was produced. This curve was then imported into an Excel spreadsheet to calculate the time (min), for the thermocouples to reach 300 °C. Subsequently, the charring rate was calculated based on the exposure depth and these times. Similar approaches to numerical modeling of timber fire resistance can be found in the literature (Thi *et al.* 2016; Zhang *et al.* 2019; Sulc *et al.* 2021). The numerical models for this study were developed using key parameters related to thermal properties and charring (EC5 2004; Bedon and Fragiacomo 2019; Pecenko and Hozjan 2020; Špilák *et al.* 2022).

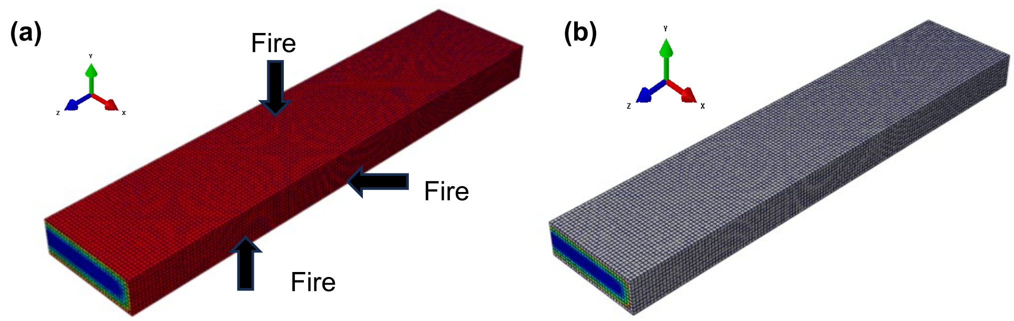

Fig. 4. Visualization of temperature contour of the model: (a) Temperature profile across the cross-section subjected to three-sided fire exposures; (b) Formation of charring layer with grey colour at 300 °C

RESULTS AND DISCUSSION

Charring Rate from Indirect Measurement from Experiments

The thermocouples data from the two-dimensional fire test for Resak were analysed to map the 300 °C isotherm through each specimen for the whole exposure time. Temperature measurements were made at various depths and positions within the beams during 60 min are shown in Fig. 5. Subsequently, Table 1 shows that the time taken for thermocouples to reach 300°C isotherm for the fire test.

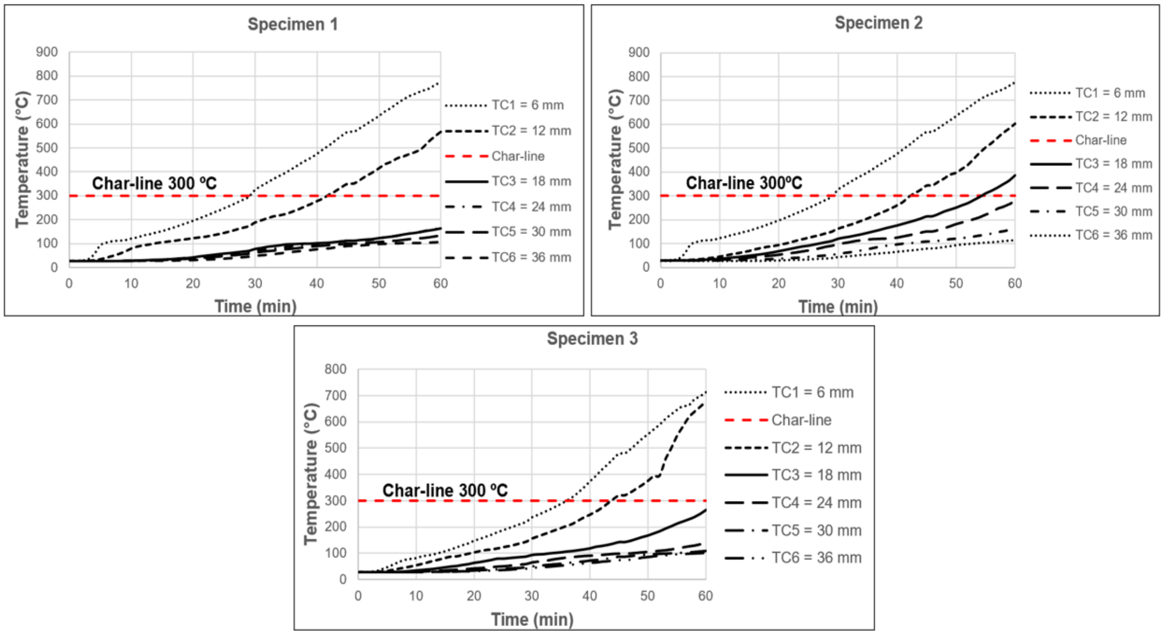

Fig. 5. Temperature-Time curve

Resak timber is expected to reach 300 °C and be able to char after 50 min of fire exposure at depth of 24 mm. The temperature recorded at gauge point TC1 shows that ignition occurred between 3 min and 5 min. This was also visually confirmed by observing the test specimen through the observation opening in the furnace wall. The temperature distributions for all specimens reveal a clear correlation between the temperatures and the placement of the thermocouples. The farther the thermocouples were from the exposed surface, the longer it took to reach the 300 °C isotherm. For the shallower thermocouples (measured from the unexposed surface), most did not reach 300 °C, as clearly presented in Table 1. Around 5 min for TC1 and 10 min for TC2, the temperature began to rise gradually, and at approximately 100 °C, a plateau was observed in the temperature-time curve for both TC1 and TC2. This plateau can be explained by the moisture in the wood, as the heat drives off the moisture in the form of steam, with 100 °C being the boiling point of water. At 300 °C, the temperature marking the char line, a depth of approximately 6 mm was affected by the fire within the first 30 min. As the char layer forms, the rate of fire penetration slowed down to a steady pace, which continued throughout the duration of the exposure. The temperature-depth profiles for Resak after 60 min of fire exposure are shown in Fig. 6.

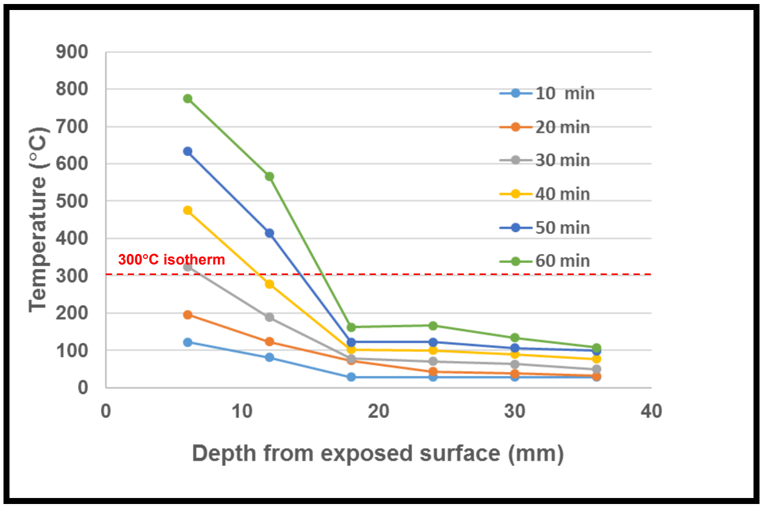

Fig. 6. Experimental Temperature-depth profiles of Resak beam measured from exposed surface

Table 1. Charring Rate from Experimental Test

Resak		TC1 (6 mm)	TC2 (12 mm)	TC3 (18 mm)	TC4 (24 mm)	TC5 (30 mm)	TC6 (36 mm)
S1 (978kg/m^3)	Time, t_{300} (min)	29.4	42.3	54.3	0.0	0.0	0.0
	$\beta_{300\ i,j}$ (mm/min)	0.20	0.47	0.5	0.0	0.0	0.0
	β_j (mm/min)	0.39					
S2 (932 kg/m^3)	Time, t_{300} (min)	29.1	41.6	0.0	0.0	0.0	0.0
	$\beta_{300\ i,j}$ (mm/min)	0.21	0.48	0.0	0.0	0.0	0.0
	β_j (mm/min)	0.34					
S3 (1125kg /m^3)	Time, t_{300} (min)	35.9	43.6	0.0	0.0	0.0	0.0
	$\beta_{300\ i,j}$ (mm/min)	0.17	0.78	0.0	0.0	0.0	0.0
	β_j (mm/min)	0.47					
Charring Rate		0.47					

The charring rate was calculated using an indirect measuring method in line with EN13381-7 (2019). By using the determined times $t300\ i,j$ in minutes, the charring rate $\beta 300\ i,j$ between 2 consecutive depths and the mean βj for all measurement stations j were assessed. The calculation of charring rate takes the following form as in Eq. 3:

$$t_{300}\ (\text{min}) = \frac{325\ °\text{C} - 296\ °\text{C}}{300\ °\text{C} - 296\ °\text{C}} = \frac{30\ min - 29\ min}{x - 29\ min} \quad (3)$$

Wood starts to char at temperatures exceeding 300 °C. Table 1 provides an example of the charring rate calculation for three (3) replicates of Resak exposed to 60 minutes of fire. The highest charring rate among the three readings was taken as the charring rate for Resak. As stated in 13.3 (b) of EN13381-7, the charring rate is the maximum of all charring rates βj which can be determined at 0.47mm/min for the actual specimen *i.e*. specimen S3. The charring rate for Resak is 0.47 mm/min, and this value is smaller than the recommended value in EC 5 (2004), which is 0.55 mm/min.

Charring Rate Through Indirect Measurement from Finite Element Model

Figure 7 presents the temperature distribution at various depths within Resak wood, as determined by numerical finite element modeling (FEM). The simulated temperature curves exhibit a trend consistent with those observed in the experimental study.

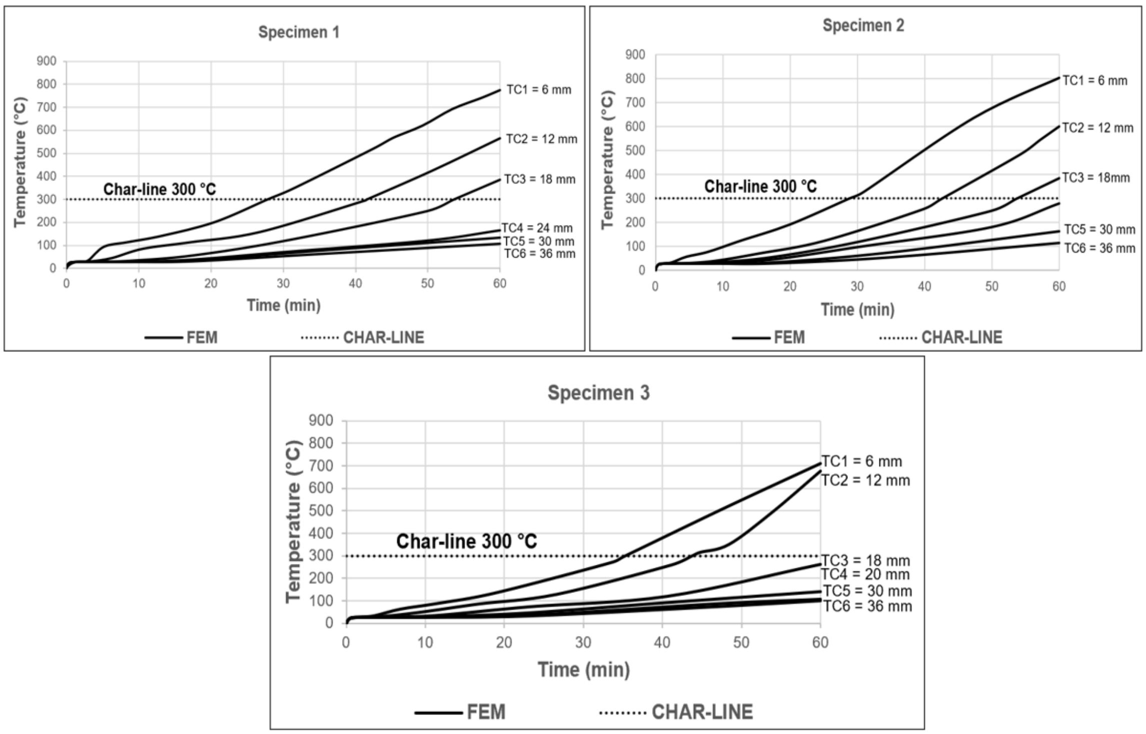

Fig. 7. FEM temperature-time relationships for Resak: a) Specimen 1 (Density 978 kg/m^3); b) Specimen 2 (Density 932 kg/m^3); and c) Specimen 3 (Density 1125 kg/m^3)

The average temperatures recorded at each thermocouple closely aligned with both the experimental results and relevant standards, with the exception of specimen S3, which showed a significantly lower charring rate in the simulation. The higher charring rate observed in S3 during experimental testing may be attributed to variations in the actual condition of the wood, such as the presence of natural defects. For S1 and S2, TC1, TC2, and TC3 were able to reach 300 °C. Meanwhile, for S3, only TC1 and TC2 exceeded 300 °C within 60 minutes. The charring rates for Resak based on the FEM simulation are presented in Table 2. The charring rate by FEM for Resak was 0.38 mm/min.

Table 2. Charring Rate by FEM

Resak		TC1 (6 mm)	TC2 (12 mm)	TC3 (18 mm)	TC4 (24 mm)	TC5 (30 mm)	TC6 (36 mm)
S1 (978kg/ m^3)	Time, t_{300} (min)	27	40.8	53	0.0	0.0	0.0
	$\beta_{300\ i,j}$ (mm/min)	0.22	0.43	0.49	0.0	0.0	0.0
	β_j (mm/min)	0.38					
S2 (932 kg/m^3)	Time, t_{300} (min)	35	42	0.0	0.0	0.0	0.0
	$\beta_{300\ i,j}$ (mm/min)	0.17	0.86	0.0	0.0	0.0	0.0
	β_j (mm/min)	0.34					
S3 (1125kg /m^3)	Time, t_{300} (min)	35.2	43.7	0.0	0.0	0.0	0.0
	$\beta_{300\ i,j}$ (mm/min)	0.17	0.71	0.0	0.0	0.0	0.0
	β_j (mm/min)	0.29					
Charring Rate (mm/min)		0.38					

Figure 8 presents the temperature distribution within a wood specimen subjected to 60 minutes of fire exposure, as simulated using the Finite Element Method (FEM) for three different depths. Each subfigure is accompanied by a color scale legend (NT11), indicating temperature values in degrees Celsius. The temperature ranged from approximately 774.9 °C (red) to below 20 °C (dark blue). The gradation from red to blue illustrates the heat penetration depth and thermal gradient within the wood specimen. As expected, the simulation of temperature contours shows the node temperature (NT) which is the temperature in the wood rises decreases towards the center of the timber cross-section element as temperature of fire exposure increases.

Figure 8a (6 mm thermocouple) reflects the highest penetration of high temperatures, with a large region reaching or exceeding 300 °C. Meanwhile, Fig. 8b, displays a more moderate heat penetration compared to Fig. 8a. The red and orange zones (indicating high-temperature regions) are shallower, implying a slower rate of heat transfer. Figure 8c exhibits the least amount of heat penetration among the three. The core remains largely within lower temperature bands (green to blue), suggesting superior fire resistance or insulation characteristics under the simulated conditions.

These simulations effectively demonstrate the variation in thermal response and charring behavior based on wood properties or boundary conditions. In all three cases, the highest temperatures were concentrated near the fire-exposed surface (left side), with a thermal gradient diminishing toward the opposite end. The extent of the red zone correlates with the depth of charring and thermal degradation. The results further indicate that the cross-sectional profile of the wood undergoes a noticeable transformation from its original rectangular shape to a more rounded contour, particularly at the corners. This deformation is attributed to the heat exposure applied under three-sided boundary conditions, which leads to differential thermal gradients and accelerated degradation at the exposed edges.

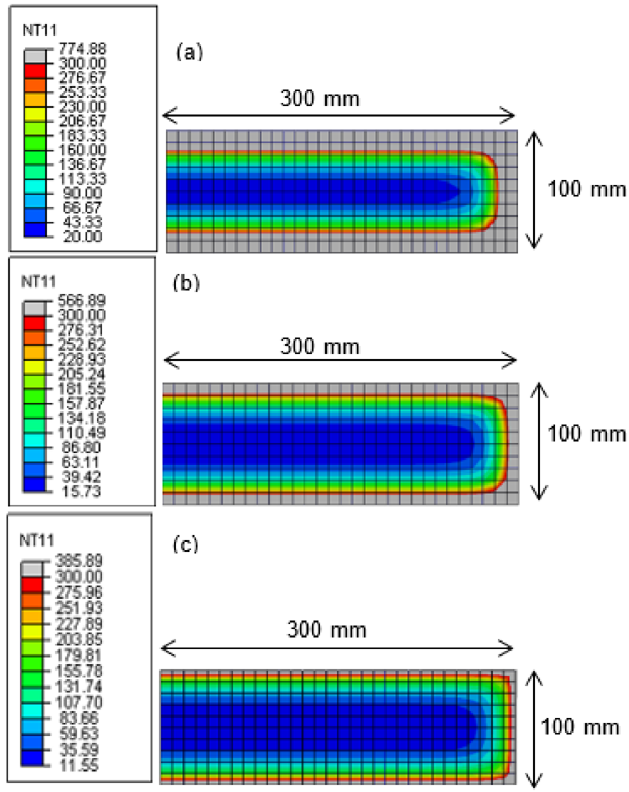

Fig. 8. X-Y View of the temperature profile and char at different depths after the thermal exposure: (a) At 6 mm exposed surface; (b) At 12 mm exposed surface; and (c) At 18 mm exposed surface

However, in accordance with the provisions outlined in EN 13381-7:2019, the phenomenon of corner rounding is not explicitly accounted for in the standard charring depth analysis. The standard assumes a uniform planar surface recession during fire exposure, thereby simplifying the geometric profile of the charred section for calculation purposes. As such, while the FEM simulation accurately captures the thermal effects leading to curvature at the corners, this detail is intentionally excluded in standard-based assessments to maintain consistency and conservatism in fire resistance evaluations.

Comparison of Charring Rate from Experimental Test and FEM

Figure 9 shows the temperature-time curve comparison for FEM and experimental of all the specimens at various depths from the exposed side of Resak for 60 min fire exposure. The numerical FEM model and experimental data were in good agreement for all thermocouples from the beginning until 60 min fire exposure. The simulated temperature distribution was almost the same as the temperature developed in the experimental test. The temperature distribution of the FEM was within the error bar upper bound and lower bound of the experimental data with small deviations, which indicated that there was good correlation between experimental and FEM data. It shows that the model was verified and accurate. This temperature observation was consistent with the established temperature-time curve outlined in the ISO 834 (2014) standard. Results show that the thermal model can simulate the temperature changes of specimens in fire tests with reasonable accuracy to reach the temperature field distribution of the timber section in the experiments.

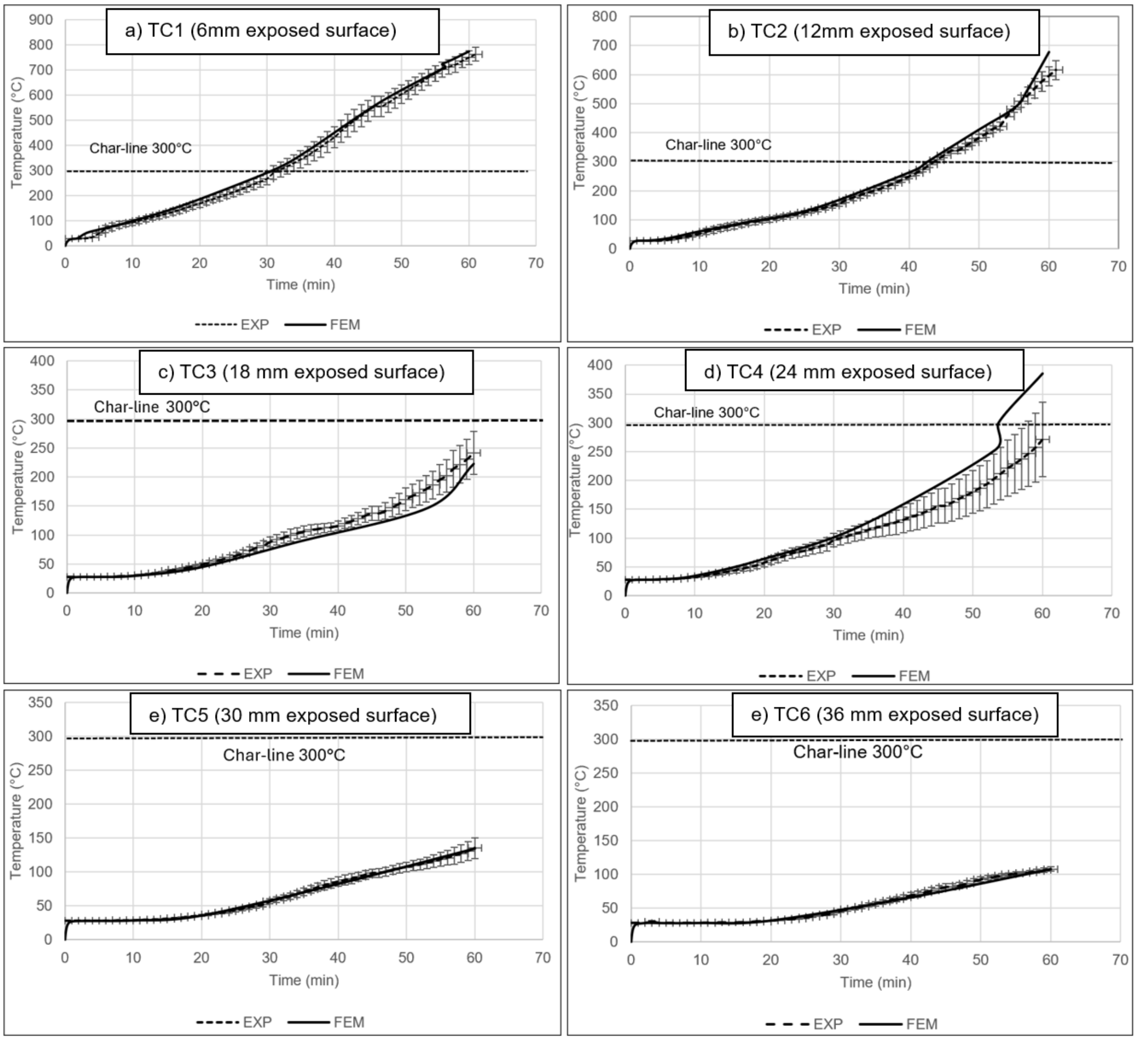

Fig. 9. Comparison of temperature distribution of FEM and experimental data

Table 3 shows the comparison of time to reach the 300 °C isotherm for different depth between FEM and experimental test. When compared with the experimental test results, the time required for thermocouples to achieve 300 °C isotherm for the model was almost similar, with only difference percentage of 2.49% for TC1, 3.54% for TC2, and 4.4% for TC3. Resak timber is expected to achieve burned temperature after 50 min of fire exposure at 18 mm depth. The thermocouples do not produce any signals at temperatures below 300 °C, indicating that the heat in that region did not reach the 300 °C isotherm.

Table 3. Time Taken for Thermocouples to Reach 300 °C Isotherm

Thermocouples	Depth (mm)	Experimental Test (min)	FEM (min)	Percentage Difference (%)
TC1	6	29.4	27	4.4%
TC2	12	42.3	40.8	3.54%
TC3	18	54.3	53	2.49%
TC4	24	Not reach	Not reach	-
TC5	30	Not reach	Not reach	-
TC6	36	Not reach	Not reach	-

The charring rate for Resak exposed to 60 min fire was 0.38 mm/min in the FEM simulation, compared to 0.47 mm/min in the experiment, according to the data shown in Table 4.

Table 4. Charring Rate by Experimental Test and FEM

	Density (kg/m^3)	Experimental (mm/min)	FEM (mm/min)	Percentage Differences (%)
S1	978	0.39	0.38	2.56%
S2	932	0.34	0.34	0%
S3	1125	0.47	0.29	6.3%
Average	1011.67	0.47	0.38	5%

There was good agreement between the FEM and experimental results, with a percentage difference of 5%. The FEM results in Fig. 8 show that the formation of a char layer on the timber sample increases as the exposed surface depth nears to the fire source, which is consistent with the experimental test. Thus, it can be concluded that the numerical model accurately predicted the charcoal layer, virtually identically to the experimental results. These results are consistent with the numerical analyses conducted by Thi *et al*. (2016), Pereira *et al.* (2024), and Trans *et al*. (2022).

The charring rate values obtained from this study were also compared with the established charring rate values. Table 5 summarizes the charring rate for this experimental work and literature data. In addition, the charring rate from EC 5 (2004) for solid hardwood timber is also included for comparison.

Table 5. Comparison of Charring Rates of Different Species and Densities of Timber

Timber Species	Density (kg/m^3)	Charring Rate (mm/min)
Resak (This experiment)	1011.67	0.47
Solid Hardwood (EC5)	≥ 450	0.5
Hardwood SG4 to SG5 (MS544 Part 9)	600 to 1000	0.70
Spruce (Scaffer 1984)	470 to 480	0.60 to 0.70
Douglas Fir (König and Walleij 1999)	300 to 500	0.63 to 0.92

When comparing the charring rate of Resak timber obtained from this experiment with reference values provided in Malaysian Standard MS544 Part 9 (2001), it is evident that Resak exhibited a significantly lower charring rate. According to MS544, timber in strength groups SG4 to SG5 with densities ranging between 600 kg/m^3 to 1000 kg/m^3 is typically assigned a charring rate of 0.70 mm/min. In contrast, Resak, which falls within the SG4 classification and has a higher density of 1012 kg/m^3, exhibited a lower charring rate of 0.47 mm/min in this study.

This trend is further supported when comparing Resak to the general classification for solid hardwoods in Eurocode 5 (EC5), which assigns a standard charring rate of 0.5 mm/min for timber with densities above 450 kg/m^3. Despite its significantly higher density, Resak still outperforms this benchmark by exhibiting a slightly lower charring rate, indicating better fire resistance.

Additionally, when compared to other species such as Spruce and Douglas Fir, which are commonly used in European and North American construction, Resak showed superior thermal performance. Both Spruce and Douglas Fir, with lower densities ranging from 300 kg/m^3 to 500 kg/m^3, report higher charring rate ranges (0.60 mm/min–0.70 mm/min and 0.63 mm/min – 0.92 mm/min respectively), highlighting the enhanced fire resistance properties of high-density tropical hardwoods like Resak.

These findings reinforce the potential suitability of Malaysian tropical hardwoods, particularly Resak, for use in fire-resistive structural applications. However, further studies across a broader range of species and under varying fire exposure conditions are recommended to generalize this conclusion.

CONCLUSIONS

This study successfully demonstrated the application of the Finite Element Method (FEM) to model the thermal behaviour of selected Malaysian tropical timber species, specifically Resak timber, under fire exposure conditions. The thermal response of the timber was evaluated through temperature distribution profiles and validated against experimental data for 60 minutes of fire exposure under three-sided heating conditions.

The simulation results showed good agreement with experimental findings, particularly in terms of temperature trends at various depths. Notably, the FEM model accurately captured the thermal gradient and heat penetration within the cross-section of the timber specimens. However, some deviations were observed, especially in the case of specimen S3, where the experimental charring rate was significantly higher. This discrepancy is likely attributable to natural variability in timber properties such as density, moisture content, and inherent defects.

The charring rate of Resak timber was found to be closely aligned with the value specified in Eurocode 5 (2004), suggesting that Malaysian tropical hardwoods possess commendable fire resistance characteristics. This observation supports the potential applicability of EC5 guidelines for local hardwood species. Specifically, the standard charring rate of 0.5 mm/min originally intended for solid timber with a density exceeding 450 kg/m^3 may be considered suitable for design applications involving Malaysian hardwoods, which typically exhibit higher characteristic densities ranging from 600 kg/m^3 to 1000 kg/m^3. Nonetheless, further experimental and numerical investigations are recommended to substantiate this preliminary conclusion and ensure its validity across different species and fire scenarios. The numerical models also revealed the tendency for corner rounding in the heated specimens, a phenomenon resulting from heat transfer at the edges under three-sided exposure. Although this effect was clearly observed in the simulations, it is not addressed in standard fire resistance assessments such as EN 13381-7:2019, which assume planar charred surfaces for simplicity.

Overall, the FEM approach proved to be an effective and reliable tool for predicting the thermal performance of tropical hardwoods in fire scenarios. The study will provide a useful foundation for further refinement of fire design methods for timber structures and highlights the importance of incorporating material-specific thermal properties in numerical modelling. Future work may include expanding the model to account for variable moisture content, anisotropic thermal behaviour, and charring kinetics for improved accuracy and wider application in performance-based fire engineering of timber.

ACKNOWLEDGMENTS

This research was funded by the Ministry of Higher Education under Fundamental Research Grant Scheme (Grant No. FRGS/1/2023/TK06/UITM/03/1) and Malaysian Timber Industry Board (MTIB). The authors also wish to thank the Fire Protection Laboratory, Forest Research Institute Malaysia (FRIM), and Research Management Centre Universiti Teknologi MARA(UiTM) for laboratory and administrative support.

REFERENCES CITED

Amin, R., Mo, Y., Richter, F., Kurzer, C., Werther, N., and Rein, G. (2024). "Predicting the average charring rate of mass timber using data-driven methods for structural calculations," *Fire Technology* 60(6), 4001-4021.

Bakri, Z., Ahmad, Z., and Ismail, S. (2023). "One-dimensional charring rate performance of laminated veneer lumber from selected Malaysian tropical timber under standard fire exposure," *International Journal of Infrastructure Research and Management* 11(S), 84-95.

Bartlett, A. I., Hadden, R. M., and Bisby, L. A. (2019). "A review of factors affecting the burning behaviour of wood for application to tall timber construction," *Fire Technology* 55(1), 1-49. DOI: 10.1007/s10694-018-0787-y

Bedon, C., and Fragiacomo, M. (2019). "Fire resistance of thermally insulated log-house timber walls," *Fire Technology* 55(1), 307-341. DOI: 10.1007/s10694- 018-0792-1

BS 476-20 (1987). "Fire tests on building materials and structures: Method for determination of the fire resistance of elements of construction," British Standards Institution, London, UK.

EN 1363-1 (2012). "Fire resistance tests — Part 1: General requirements," European Committee for Standardization, Brussels, Belgium.

EN 1995-1-2 (2004). "Eurocode 5: Design of timber structures — Part 1-2: General — structural fire design," European Committee for Standardization, Brussels, Belgium.

EN 13381-7 (2019). "Test methods for determining the contribution to the fire resistance of structural members," European Committee for Standardization, Brussels, Belgium.

Frangi, A., Erchinger, C., and Fontana, M. (2008). "Charring model for timber frame floor assemblies with void cavities," *Fire Safety Journal* 43(8), 551-564. DOI: 10.1016/j.firesaf.2007.12.009

ISO 834 (2014). "Fire resistance tests. Elements of building construction, Part 11: Specific requirements for the assessment of fire protection to structural steel elements," International Organization for Standardization, Geneva, Switzerland.

Jabar, K. A. (2023). "Charring rate of Kelempayan (*Neolamarckia cadamba*)," in: *Proceedings of the Forest Products Seminar Lignocellulosic Materials Towards a Sustainable Future*, Forest Products Division of the Forest Research Institute Malaysia.

Khelifa, M., Thi, V. D., Oudjène, M., Khennane, A., El Ganaoui, M., and Rogaume, Y. (2024). "Modelling the response of timber beams under fire," *International Journal of Civil Engineering* 22, 1537-1549. DOI: 10.1007/s40999-024-00973-2

König, J., and Walleij, L. (1999). *One-dimensional Charring of Timber Exposed to Standard and Parametric Fires in Initially Unprotected and Post Protection*

Situations (Rapport1: 9908029), Swedish Institute for Wood Technology Research, Trätek, Sweden.

Li, Q., Xu, B., Chen, K., Cui, Z., Liu, Y., and Zhang, L. (2024). "Experimental and three-dimensional numerical investigations of dehydration and pyrolysis in wood under elevated and high temperatures," *Buildings* 14(6), article 1547. DOI: 10.3390/buildings14061547

Li, X., Zhang, X., Hadjisophocleous, G., and McGregor, C. (2015). "Experimental study of combustible and non-combustible construction in a natural fire," *Fire Technology* 51(6), 1447-1474. DOI: 10.1007/s10694-014-0407-4

Liu, J., and Fischer, E. C. (2024). "Review of the charring rates of different timber species," *Fire and Materials* 48(1), 3-15. DOI: 10.1002/fam.3173

MS 544 Part 9 (2001). "Code of practice for structural use of timber - Part 9: Fire resistance of timber structures: Section 1: Method of calculating fire resistance of timber members," Department of Standards Malaysia, Cyberjaya, Malaysia.

MS 1714 (2003). "Specification of visual strength grading of tropical hardwood timber," Department of Standards Malaysia, Cyberjaya, Malaysia.

Pečenko, R., Hozjan, T., and Huč, S. (2023). "Modelling charring of timber exposed to natural fire," *Journal of Wood Science* 69(1), article 19. DOI: 10.1186/s10086-023-02091-4

Peˇcenko, R., and Hozjan, T. (2020). "A novel approach to determine charring of wood in natural fire implemented in a coupled heat-mass pyrolysis model," *Holzforschung* 75, 148-158. DOI: 10.1515/hf-2020-0081

Pereira, D., Fonseca, E. M., and Osório, M. (2024). "Computational analysis for the evaluation of fire resistance in constructive wooden elements with protection," *Applied Sciences* 14(4), article 1477. DOI: 10.3390/app14041477

Scaffer, E. L. (1984). *Structural Fire Design: Wood- Transverse to Grain* (Res. Rap. FPL 450), Department of Agriculture, Forest Product Laboratory, Madison, WI, USA.

Shi, L., and Chew, M. Y. (2023). "A review of thermal properties of timber and char at elevated temperatures," *Indoor and Built Environment* 32(1), 9-24. DOI: 10.1177/1420326X211035557

Špilák, D., Majlingová, A., Kaˇcíková, D., and Tischler, P. (2022). "Determining the charred layer of wooden beams with finite element analysis based on enthalpy approach," *Buildings* 12(7), article 875. DOI: 10.3390/buildings12070875

Suzuki, J. I., Mizukami, T., Naruse, T., and Araki,Y. (2016). "Fire resistance of timber panel structures under standard fire exposure," *Fire Technology* 52(4), 1015-1034. DOI: 10.1007/s10694-016-0578-2

Šulc, S., Šmilauer, V., and Wald, F. (2021). "Thermal model for timber fire exposure with moving boundary," *Materials* 14(3), article 574. DOI: 10.3390/ma14030574

Thi, V. D., Khelifa, M., El Ganaoui, M., and Rogaume, Y. (2016). "Finite element modelling of the pyrolysis of wet wood subjected to fire," *Fire Safety Journal* 81, 85-96. DOI: 10.1016/j.firesaf.2016.02.001

Tran, T. T., Thi, V. D., Oudjene, M., Khelifa, M., Girods, P., Debal, M., and Jannot, Y. (2022). "Fire structural performance of thermo-mechanically compressed spruce timber by means experiments and a three-step multi-reactions pyrolysis 3D-finite element modelling," *Construction and Building Materials* 320, article 126100. DOI: 10.1016/j.conbuildmat.2021.126100

UBBL (1984). *Uniform Building By-Laws*, Laws of Government Malaysia, Malaysia.

White, R. H., and Dietenberger, M. A. (2001). "Wood products: Thermal degradation and fire," *Encyclopedia of Materials: Science and Technology*, Elsevier Science Ltd., Amsterdam, Netherlands, pp. 9712-9716.

Zhang, Y., Zhang, L., Shan, Z., Wang, L., and Liu, W. (2019). "Thermal responses of woods exposed to high temperatures considering apparent thermo-physical properties," *Journal of Renewable Materials* 7(11), 1095-1110. DOI: 10.32604/jrm.2019.07335

Article submitted: November 15, 2024; Peer review completed: February 22, 2025; Revised version received: July 19, 2025; Accepted: July 21, 2025; Published: July 28, 2025.

DOI: 10.15376/biores.20.3.7695-7712